

DOMAIN INTEGRALS FOR AXISYMMETRIC INTERFACE CRACK PROBLEMS

R. NAHTA and B. MORAN

Department of Civil Engineering, Northwestern University, 2145 Sheridan Road,
Evanston, IL 60208, U.S.A.

(Received 7 August 1992; in revised form 8 January 1993)

Abstract—New domain integrals for axisymmetric interface crack problems are derived. Special attention is given to the specification and subsequent treatment of auxiliary fields for the extraction of mixed-mode stress intensity factors using interaction energy integrals. The effect of crack front curvature is shown to play an important role in the derivation of the integrals. Numerical examples include an interface penny-shaped crack and a longitudinal interface crack (fiber pull-out problem), and yield very accurate and consistent results, when compared with analytical solutions from the literature. The method is particularly suited for the analysis of fiber pull-out experiments and the accurate determination of fracture-parameters such as energy release rate G , mixed-mode stress-intensity factors K_I and K_{II} and phase angle ψ .

1. INTRODUCTION

For wide classes of problems in fracture mechanics, the parameters characterizing the crack-tip fields (critical values of which may form the basis of a fracture criterion) can be represented in terms of crack-tip contour integrals. Under certain conditions, these contour integrals are path-independent conservation integrals, otherwise they are only defined in a limiting sense as the contour is shrunk onto the crack tip. A particularly useful method for the evaluation of such crack-tip integrals is the so-called domain integral method wherein the crack-tip integral is represented as an integral over a finite domain surrounding the crack tip. A general discussion of crack-tip contour integrals and their associated domain integral representations has been given by Moran and Shih (1987a, b). The domain integral method was used to evaluate the energy release rate along a three-dimensional crack front by Li *et al.* (1985) and Shih *et al.* (1986). Nikishkov and Atluri (1987) employed the domain integral procedure for the evaluation of mixed-mode stress-intensity factors for an arbitrary three-dimensional crack using vector components of the J -integral. Shih and Asaro (1988) used domain integral representations of interaction energy integrals for the extraction of mixed-mode stress-intensity factors for planar bimaterial crack problems. Nakamura (1991) used the same procedure to evaluate mixed-mode stress intensity factors along a three-dimensional interface crack and Nakamura and Parks (1992) illustrated how the method may be employed in the evaluation of the elastic T -stress along a three-dimensional crack front.

Axisymmetric crack problems arise in many aspects of fracture mechanics. Crack configurations that fall into this category include penny-shaped cracks, circumferentially cracked cylinders and fiber pull-out problems. However, due to the underlying three-dimensionality manifested through curvature effects and hoop terms, axisymmetric crack problems yield crack-tip integrals that are not path-independent even if the corresponding planar integral is. Appropriate domain integral representations of the J -integral for penny-shaped crack problems have been given by Moran and Shih (1987a). In this paper, we consider axisymmetric interface crack problems and introduce appropriate interaction energy integrals and their associated domain-integral representations for the extraction of mixed-mode stress-intensity factors.

Charalambides and Evans (1989) studied the problem of interface debonding in a fiber pull-out test. They used the stiffness derivative method to compute the energy release rate, G , and phase angle, ψ , and noted that difficulties arise in the specification of auxiliary fields in the extraction of mixed-mode stress-intensity factors. In particular, their formulation only permits the specification of the auxiliary fields in the immediate vicinity of the crack

tip, a restriction which may lead to a loss of accuracy. This difficulty is eliminated in the domain integral formulation presented here. Furthermore, the reasons for the difficulties encountered with the stiffness derivative method are illustrated and implications for the evaluation of stress-intensity factors in three-dimensional curved (interface) crack problems are discussed.

In the following section, a preliminary discussion of crack-tip integrals and their axisymmetric specializations is given. A brief description of the pertinent aspects of interface fracture mechanics is given in Section 3. In Section 4, interaction energy integrals for the extraction of mixed-mode stress-intensity factors in interface crack problems are introduced. Axisymmetric specializations are then discussed and in particular the choice of auxiliary fields is motivated. A noteworthy feature of the method is that the most suitable auxiliary fields are neither equilibrated nor compatible and this plays an important role in the derivation of the domain integral representations. In Section 5, numerical examples for both penny-shaped and longitudinal (fiber pull-out) crack problems are presented and compared with analytical solutions from the literature. Some concluding remarks are presented in Section 6 and implications for extension of the present approach to curved three-dimensional interface crack problems are discussed.

2. GENERAL CRACK-TIP INTEGRALS

As a point of departure for the present paper, we consider the expression for a general crack-tip integral along a three-dimensional crack front [see Moran and Shih (1987a, b), for example]. Referring to Fig. 1, the general integral takes the form

$$I(s) = \lim_{\Gamma \rightarrow 0} \xi_j(s) \int_{\Gamma(s)} P_{i,j} n_i d\Gamma. \quad (1)$$

In the spirit of general energetic or interaction energy integrals, $\xi_i(s)$ is the local defect translation (crack extension) and $\Gamma(s)$ is a crack-tip contour in the local x_1 - x_2 plane at a point s on the crack front. For example when the integral pertains to energy release rate due to crack extension in its own plane, $P_{i,j} = W\delta_{ij} - \sigma_{ij}u_{i,j}$ which is the energy-momentum tensor (Eshelby, 1956, 1970) and $\xi_j(s)$ is the unit normal to the crack front in the local tangent plane to the crack faces. Here W is the strain energy density, σ_{ij} is the stress, u_i the displacements and a comma denotes a partial derivative with respect to the coordinates. In the case of interaction integrals for the extraction of mixed-mode stress-intensity factors in interface crack problems, the appropriate form for plane problems is given by Shih and Asaro (1988) while that for three-dimensional (straight) interface cracks is given by Nakamura (1991). A similar approach for the determination of the elastic T -stress in three-dimensional crack problems is adopted by Nakamura and Parks (1992). Note that the integral (1) is, in general, only asymptotically path-independent and requires the limit $\Gamma \rightarrow 0$.

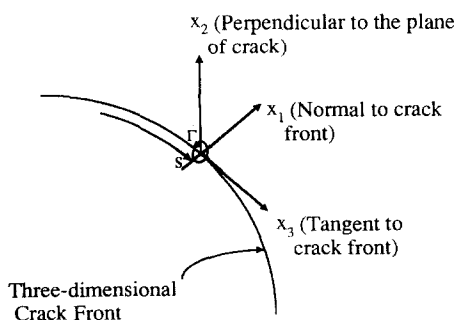


Fig. 1. Local coordinate system (x_1, x_2, x_3) at a point s on a curved crack front.

The so-called domain integral method [see Li *et al.* (1985), Shih *et al.* (1986) and Moran and Shih (1987a, b), for example] can be used to represent the integral (1) in a form more suited to numerical computation. Introducing a weighting function q_ℓ where $q_\ell = \xi_\ell$ on the crack-tip contour $\Gamma(s)$ and is extended smoothly to the domain V vanishing on the remote boundary of V , we obtain the domain/volume integral

$$\begin{aligned} \bar{I}(s) &= \int_{L_c} I(s') ds' = - \int_{V(s)} (P_{\ell j} q_{i,j} + P_{\ell j,j} q_\ell) dV \\ &= - \int_{V(s)} [\text{tr}(\mathbf{P} \cdot \nabla \mathbf{q}) + (\nabla \cdot \mathbf{P}^T) \cdot \mathbf{q}] dV, \end{aligned} \tag{2}$$

where L_c is a small crack front segment centered at s . Here we have assumed the absence of crack face tractions/fluxes which can be readily incorporated as described by Shih *et al.* (1986), for example. When the tensor \mathbf{P}^T is divergence-free (e.g. no body force, thermal strains, inertia, etc.), the second term in the integrand vanishes. In plane problems, the crack-tip integral (1) is thus globally path-independent. In the three-dimensional (and hence axisymmetric) case, local or asymptotic path-independence only is obtained.

As an example, consider the energy release rate for plane strain crack extension in an elastic body (with \mathbf{P}^T divergence-free). Crack extension is assumed to be in the plane of the crack and in the x_1 -direction of the local coordinate system shown in Fig. 1. Thus, $\xi_\ell = \delta_{1\ell}$ and $q_\ell = q(x_1, x_2) \delta_{1\ell}$ where again $q_\ell = \xi_\ell$ on Γ . The crack segment is taken to be unit length (in the x_3 -direction) and using (1) and (2) we obtain

$$\bar{I} = I \equiv J = - \int_A (W \delta_{1j} - \sigma_{ij} u_{i,1}) q_j dA, \tag{3}$$

where A is the area bounded by Γ , the crack faces and the remote contour C as shown in Fig. 2.

2.1. Axisymmetric specialization

Taking the crack front segment L_c to be the whole axisymmetric crack front and taking account of the axisymmetry we have $\bar{I} = 2\pi R I$ and thus (2) can be written as

$$I = - \frac{1}{R} \int_A [\text{tr}(\mathbf{P} \cdot \nabla \mathbf{q}) + (\nabla \cdot \mathbf{P}^T) \cdot \mathbf{q}] r dA, \tag{4}$$

where R is the crack radius. Note that $\nabla \cdot \mathbf{P}^T$ would be zero, in the absence of body forces, thermal strains, inertia and inhomogeneity.

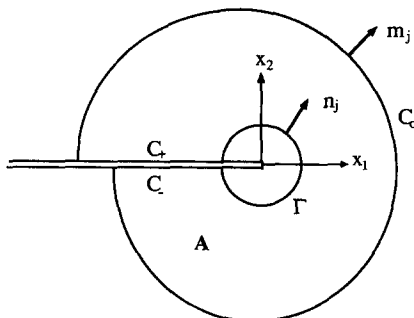


Fig. 2. Conventions at crack tip. Domain A is enclosed by Γ , C_+ , C_- and C_0 .

Energy release rate for penny-shaped crack. Following Moran and Shih (1987a) the expression for the energy release rate along a penny-shaped crack front is obtained from (4) by letting \mathbf{P} be the energy-momentum tensor, introducing polar coordinates, as shown in Fig. 3(a), and choosing $\xi = \mathbf{e}_r$ and $\mathbf{q} = q(r, z)\mathbf{e}_r$ to yield

$$J = \frac{1}{R} \int_A \left[(\sigma_{\gamma\beta} u_{\gamma,r} - W \delta_{r\beta}) q_{,\beta} + \left(\frac{u_r}{r} \sigma_{\theta\theta} - W \right) \frac{q}{r} - p_r q \right] r \, dr \, dz, \quad (5)$$

where Greek subscripts range over r and z and $p_r = (\nabla \cdot \mathbf{P}^T) \cdot \mathbf{e}_r$. Note that even if $p_r = 0$ in

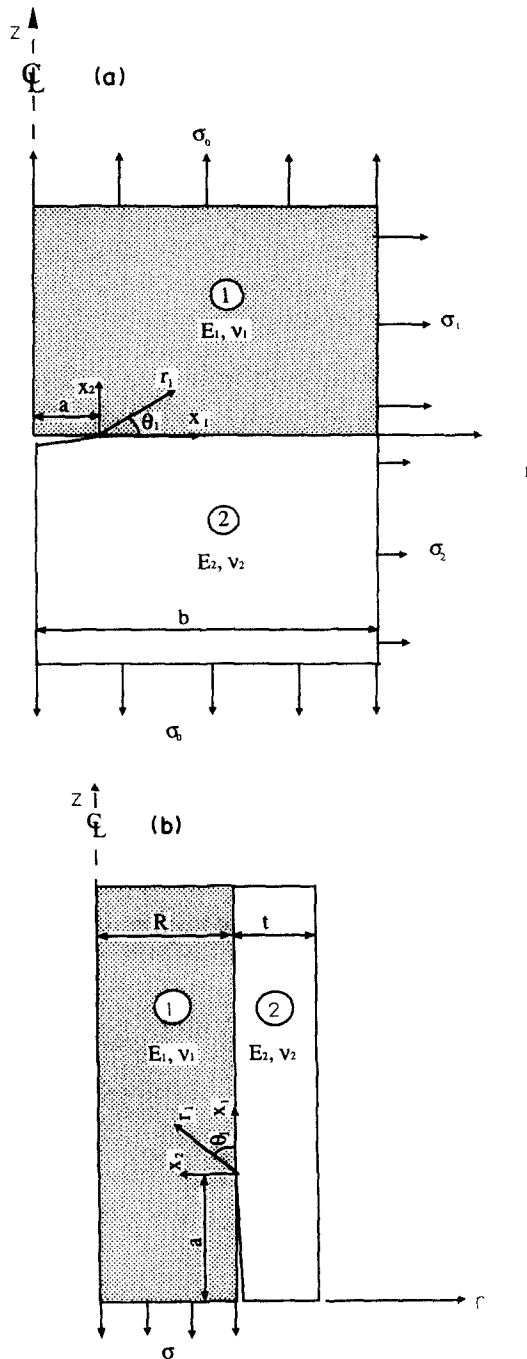


Fig. 3. (a) Axisymmetric penny-shaped interface crack under remote tension σ_0 , and (b) axisymmetric longitudinal interface crack.

the above, the corresponding crack-tip integral is not (globally) path-independent due to both the explicit curvature terms [multiplied by q/r in (5)] and the implicit hoop terms in W .

Energy release rate for longitudinal crack. An expression for the energy release rate along an axisymmetric longitudinal crack front as found, for example, in fiber pull-out problems [see Fig. 3(b)] can be obtained in a similar fashion and is introduced here. Let $\xi = \mathbf{e}_z$ and $\mathbf{q} = q(r, z)\mathbf{e}_z$ and (2) now yields

$$J = \frac{1}{R} \int_A [(\sigma_{\gamma\beta} u_{\gamma,z} - W \delta_{z\beta}) q_{,\beta} - p_z q] r \, dr \, dz. \tag{6}$$

Again, even if $p_z = 0$ in this expression, the corresponding contour integral is not (globally) path-independent due to the implicit curvature and hoop terms in W . The above expression proves to be an extremely useful one for the accurate and efficient determination of energy release rates for fiber pull-out and debond problems as will be illustrated in Section 5 below.

3. INTERFACE FRACTURE MECHANICS

A brief description and definition of the pertinent quantities for the characterization of fracture in interface crack problems is presented here in anticipation of the derivation of axisymmetric interaction integrals for interface cracks in the following section. For a more thorough description see the review articles by Rice (1988), Shih (1990) and Hutchinson and Suo (1991). Introducing a local coordinate system at the crack front as shown in Fig. 4, the near-tip field at an interface crack between dissimilar isotropic materials (Rice *et al.*, 1990) can be written as

$$\sigma_{ij} = \frac{1}{\sqrt{2\pi r_1}} \{ \text{Re} [\mathbf{K} r_1^{\epsilon}] \tilde{\sigma}_{ij}^I(\theta_1; \epsilon) + \text{Im} [\mathbf{K} r_1^{\epsilon}] \tilde{\sigma}_{ij}^{II}(\theta_1; \epsilon) + K_{III} \tilde{\sigma}_{ij}^{III}(\theta_1) \}, \tag{7}$$

where (r_1, θ_1) are polar coordinates centered at the crack tip in the plane normal to the crack front, $\mathbf{K} = K_I + iK_{II}$ is the complex stress intensity factor, $\tilde{\sigma}_{ij}$ are universal angular functions which depend on the bimaterial constant ϵ .

The interface traction vector

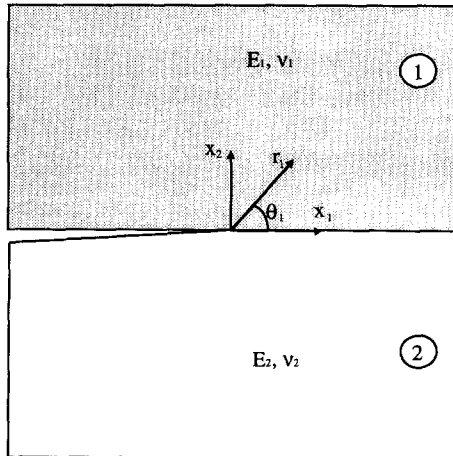


Fig. 4. Schematic diagram of a bimaterial interface crack.

$$\mathbf{t} = \sigma_{22}(r_1, 0) + i\sigma_{12}(r_1, 0)$$

is given by

$$\mathbf{t} = \frac{\mathbf{K}r_1^{ie}}{\sqrt{2\pi r_1}}. \quad (8)$$

The mode mixity (phase angle) for a reference length L is defined through

$$\mathbf{K}L^{ie} = |\mathbf{K}| \exp(i\psi), \quad (9)$$

or

$$\psi = \arctan \left[\frac{\text{Im}(\mathbf{K}L^{ie})}{\text{Re}(\mathbf{K}L^{ie})} \right]. \quad (10)$$

The physical interpretation of the phase angle ψ is that it is a measure of the ratio of shear to normal in-plane tractions at a distance L ahead of the crack tip, i.e.

$$\mathbf{t} = \sigma_{22}(L, 0) + i\sigma_{12}(L, 0) = \frac{\mathbf{K}L^{ie}}{\sqrt{2\pi r_1}} = |\mathbf{t}| \exp(i\psi) \quad (11)$$

and thus

$$\psi = \arctan \frac{\sigma_{12}(L, 0)}{\sigma_{22}(L, 0)}. \quad (12)$$

The phase angle ψ plays an important role in the characterization of interface fracture toughness.

Now introduce the Kolosov constants

$$\begin{aligned} \kappa_i &= 3 - 4\nu_i && \text{Plane Strain,} \\ &= \frac{3 - 4\nu_i}{1 + \nu_i} && \text{Plane Stress,} \end{aligned} \quad (13)$$

where i ranges over 1 and 2 and designates materials 1 and 2 respectively and ν_i and μ_i are Poisson's ratios and shear moduli respectively. Dundurs' constants can thus be written as

$$\begin{aligned} \alpha &= \frac{\mu_1(\kappa_2 + 1) - \mu_2(\kappa_1 + 1)}{\mu_1(\kappa_2 + 1) + \mu_2(\kappa_1 + 1)}, \\ \beta &= \frac{\mu_1(\kappa_2 - 1) - \mu_2(\kappa_1 - 1)}{\mu_1(\kappa_2 + 1) + \mu_2(\kappa_1 + 1)}, \end{aligned} \quad (14)$$

and the bimaterial constant ε is written as

$$\varepsilon = \frac{1}{2\pi} \ln \left[\frac{1 - \beta}{1 + \beta} \right]. \quad (15)$$

The energy release rate G is given by

$$G = \frac{1}{E^*} \frac{\mathbf{K}\bar{\mathbf{K}}}{\cosh^2(\pi\varepsilon)} + \frac{K_{III}^2}{2\mu^*}, \quad (16)$$

where

$$\frac{2}{E^*} = \frac{1}{E'_1} + \frac{1}{E'_2}, \quad \frac{2}{\mu^*} = \frac{1}{\mu_1} + \frac{1}{\mu_2}, \tag{17}$$

and

$$\begin{aligned} E' &= E/(1-\nu^2) && \text{Plane Strain,} \\ &= E && \text{Plane Stress.} \end{aligned} \tag{18}$$

4. INTERACTION ENERGY INTEGRALS

Interaction energy integrals have been used by Shih and Asaro (1988) to determine mixed-mode stress-intensity factors for interface cracks in two dimensions. The three-dimensional case has been considered by Nakamura (1991). Nakamura and Parks (1992) have also employed an interaction integral approach together with a domain integral formulation to determine the elastic *T*-stress (which plays a role in crack path stability) along a three-dimensional crack front.

For purposes of the present discussion, we first consider interaction energy integrals for a three-dimensional interface crack. The pointwise interaction energy integral for three-dimensional elastic crack problems can be cast in the form (1) by setting

$$P_{\ell j} = \sigma_{ik} \varepsilon_{ik}^{\text{aux}} \delta_{\ell j} - \sigma_{ij} u_{i,\ell}^{\text{aux}} - \sigma_{ij}^{\text{aux}} u_{i,\ell}, \tag{19}$$

where σ_{ij}^{aux} , $\varepsilon_{ij}^{\text{aux}}$ and u_i^{aux} are auxiliary stress, strain and displacement fields respectively. Letting ξ_1 be the unit normal to the crack front in the crack plane, then in the limit $\Gamma \rightarrow 0$ the interaction integral (1) becomes

$$I(s) = \frac{2}{E^* \cosh^2(\pi\varepsilon)} [K_I K_I^{\text{aux}} + K_{II} K_{II}^{\text{aux}}] + \frac{1}{\mu^*} K_{III} K_{III}^{\text{aux}}, \tag{20}$$

where K_I^{aux} , K_{II}^{aux} and K_{III}^{aux} are local stress intensity factors for the auxiliary fields. As discussed by Shih and Asaro (1988) and Nakamura (1991) we extract the individual stress intensity factors by judicious choice of the auxiliary fields. For example, to extract K_I we set $K_I^{\text{aux}} = 1$, $K_{II}^{\text{aux}} = 0$ and $K_{III}^{\text{aux}} = 0$ from which it follows that

$$K_I(s) = \frac{E^* \cosh^2(\pi\varepsilon)}{2} I(s) \tag{21}$$

and similarly for the other modes.

We note that the integral (1) is defined pointwise along the crack front in the limit $\Gamma \rightarrow 0$ where Γ lies in the local x_1-x_2 plane (Fig. 1). Hence, in developing a suitable integral for extraction of the mixed-mode stress-intensity factors, we need only retain the asymptotic terms in the auxiliary fields such that (20) is satisfied and local (or asymptotic) path-independence is maintained. As a point *s* of the curved crack front is approached in the local x_1-x_2 plane, the near-tip three-dimensional fields asymptote to the plane and antiplane strain fields (7). Therefore, the auxiliary fields in the integrand (19) of the interaction integral (1) may be defined as the plane strain (with amplitudes K_I^{aux} and K_{II}^{aux}) and antiplane (with amplitude K_{III}^{aux}) fields in the local x_1-x_2 plane. However, a consequence of imposing the plane strain asymptotic fields along a curved crack front, is that the auxiliary stress fields do not satisfy equilibrium and the auxiliary strain fields do not satisfy compatibility (strain-displacement relations). However, in the asymptotic limit $\Gamma \rightarrow 0$, terms which arise due to the lack of equilibrium and compatibility are not sufficiently singular to contribute to the crack-tip interaction integral or to affect its path-independence. Thus, the crack-tip integral is locally or asymptotically path-independent (Moran and Shih, 1987b) as desired. It is emphasized however, that the lack of equilibrium and compatibility of the auxiliary fields will emerge when domain integral representations of the integrals are derived below since these involve fields which are not asymptotically close to the crack tip.

4.1. *Axisymmetric specializations*

4.1.1. *Auxiliary fields.* The auxiliary fields for the axisymmetric problem defined with the aid of a local coordinate system which is shown in Figs 3(a), (b) for the penny-shaped and longitudinal cracks, respectively are obtained from (7).

Penny-shaped crack

$$\begin{aligned} \sigma_{rr}^{aux} &= \sigma_{11}^{aux}, & \sigma_{rz}^{aux} &= \sigma_{12}^{aux}, & \sigma_{zz}^{aux} &= \sigma_{22}^{aux}, & \sigma_{\theta\theta}^{aux} &= \sigma_{33}^{aux}, \\ \epsilon_{rr}^{aux} &= \epsilon_{11}^{aux}, & \epsilon_{rz}^{aux} &= \epsilon_{12}^{aux}, & \epsilon_{zz}^{aux} &= \epsilon_{22}^{aux}, & \epsilon_{\theta\theta}^{aux} &= \epsilon_{33}^{aux} = 0, \\ u_r^{aux} &= u_1^{aux}, & u_z^{aux} &= u_2^{aux}. \end{aligned} \tag{22}$$

Longitudinal crack

$$\begin{aligned} \sigma_{rr}^{aux} &= \sigma_{22}^{aux}, & \sigma_{rz}^{aux} &= -\sigma_{21}^{aux}, & \sigma_{zz}^{aux} &= \sigma_{11}^{aux}, & \sigma_{\theta\theta}^{aux} &= \sigma_{33}^{aux}, \\ \epsilon_{rr}^{aux} &= \epsilon_{22}^{aux}, & \epsilon_{rz}^{aux} &= -\epsilon_{21}^{aux}, & \epsilon_{zz}^{aux} &= \epsilon_{11}^{aux}, & \epsilon_{\theta\theta}^{aux} &= \epsilon_{33}^{aux} = 0, \\ u_r^{aux} &= -u_2^{aux}, & u_z^{aux} &= -u_1^{aux}. \end{aligned} \tag{23}$$

4.1.2. *Domain integral representations.* As mentioned above, the auxiliary fields employed in plane or three-dimensional crack problems can be conveniently chosen as the plane strain asymptotic fields. In employing the plane strain fields in the local coordinate system to the crack front, we preserve the asymptotic form of the fields necessary to extract the mixed-mode stress-intensity factors. However, in the process we violate both compatibility and equilibrium outside of the immediate crack-tip region. As will be seen below, the divergence \mathbf{p} of the interaction energy tensor \mathbf{P}^I will not vanish, resulting in additional contributions to the domain integral forms of the pertinent interaction integrals. This is quite different from plane problems or three-dimensional problems with straight crack fronts where, in the absence of body forces, thermal strains, inertia, etc., the interaction energy tensor is divergence-free. This qualitative difference is due to the crack front curvature and the definition of the auxiliary fields in the local coordinate system. It should be noted that, in the above definitions of the auxiliary fields, the constitutive relation is satisfied, i.e. $\sigma_{ij}^{aux} = C_{ijkl} \epsilon_{kl}^{aux}$. However, both equilibrium and compatibility (strain-displacement relationship) are violated in V or A in the r - z plane. In the absence of body forces, thermal strains, inertia, etc., the term $\mathbf{p} = \nabla \cdot \mathbf{P}^I$ would be zero, provided the auxiliary fields are equilibrated, compatible and satisfy the constitutive relation. Since only the latter is satisfied, a non-zero divergence is obtained.

Taking the divergence of \mathbf{P} , and noting the lack of equilibrium and compatibility (of the auxiliary fields) we obtain the following general expression for \mathbf{p}

$$\mathbf{p} = \sigma : (\nabla \epsilon^{aux} - \nabla \nabla \mathbf{u}^{aux}) - (\nabla \mathbf{u})^T \cdot (\nabla \cdot \sigma^{aux}). \tag{24}$$

Specializing the above to the axisymmetric case gives

$$\mathbf{p} = -\frac{1}{r} \left(\sigma_{rz}^{aux} u_{z,\beta} - \sigma_{\theta\theta}^{aux} u_{r,\beta} + \sigma_{\theta\theta} r \left(\frac{u_r^{aux}}{r} \right)_{,\beta} \right) \mathbf{e}_\beta. \tag{25}$$

Here r is the local radius of curvature of the polar coordinate system. Note that in plane problems, or three-dimensional problems with *straight* crack fronts, a single Cartesian coordinate system can be chosen wherein $r \rightarrow \infty$ and thus \mathbf{p} vanishes.

The interaction energy integrals for the axisymmetric crack configuration are thus given by (4) with \mathbf{P} given by (19), the auxiliary fields as specified in (22) and (23) and \mathbf{p} given by (24) above. For completeness the resulting integrals are :

Penny-shaped crack

$$I = -\frac{1}{R} \int_A \left[(\sigma_{\gamma\beta} u_{\gamma,r}^{\text{aux}} + \sigma_{\gamma\beta}^{\text{aux}} u_{\gamma,r} - \sigma_{ik} \epsilon_{ik}^{\text{aux}} \delta_{r\beta}) q_{,\beta} + \left(\frac{u_r}{r} \sigma_{\theta\theta}^{\text{aux}} + \frac{u_r^{\text{aux}}}{r} \sigma_{\theta\theta} - \sigma_{ik} \epsilon_{ik}^{\text{aux}} \right) \frac{q}{r} - p_r q \right] r \, dA, \quad (26)$$

where

$$p_r = -\frac{1}{r} \left[\sigma_{r\alpha}^{\text{aux}} u_{\alpha,r} - \sigma_{\theta\theta}^{\text{aux}} u_{r,r} + \sigma_{\theta\theta} \left(u_{r,r} - \frac{u_r^{\text{aux}}}{r} \right) \right]. \quad (27)$$

Longitudinal crack

$$I = -\frac{1}{R} \int_A [(\sigma_{\gamma\beta} u_{\gamma,z}^{\text{aux}} + \sigma_{\gamma\beta}^{\text{aux}} u_{\gamma,z} - \sigma_{ik} \epsilon_{ik}^{\text{aux}} \delta_{z\beta}) q_{,\beta} - p_z q] r \, dA, \quad (28)$$

where

$$p_z = -\frac{1}{r} [\sigma_{r\alpha}^{\text{aux}} u_{\alpha,z} - \sigma_{\theta\theta}^{\text{aux}} u_{r,z} + \sigma_{\theta\theta} u_{r,z}^{\text{aux}}]. \quad (29)$$

The domain integrals (26) and (28) above yield the stress intensity factors for the case of an axisymmetric penny-shaped or longitudinal crack respectively, by appropriate choice of the auxiliary fields as discussed above [see (22) and (23) in particular]. The integrals can be readily implemented into the post-processing stage of any standard finite element program or used in conjunction with boundary element solutions which have been obtained over the domain of interest. Details of the finite element implementation of the domain integrals are given in Shih *et al.* (1986) and are omitted here.

5. NUMERICAL EXAMPLES

In this section, some numerical examples are presented to illustrate the accuracy and utility of the domain integrals (26) and (28) above and comparison with analytical results is made.

5.1. *Penny-shaped interface crack under remote tension*

Consider a penny-shaped interface crack under remote tension σ_0 . For a crack of radius a in an infinite body, a closed form analytical expression for the stress intensity factors has been given by Kassir and Bregman (1972) as

$$K_I + iK_{II} = 2\sigma_0 \sqrt{a} \frac{\Gamma(1+i\epsilon)}{\Gamma(\frac{1}{2}+i\epsilon)} (2a)^{i\epsilon}, \quad (30)$$

where Γ is the Gamma function. In the numerical simulation of this problem, the crack size is kept small with respect to the overall dimensions and for the finite element mesh used $a/b = 0.02$ [see Fig. 3(a)]. For the corresponding plane strain problem in a homogeneous medium the stress-intensity correction factor for this ratio is negligible.

The material properties are chosen as those corresponding to steel ($E = 3 \times 10^7$ psi, $\nu = 0.3$) bonded to glass ($E = 1 \times 10^7$ psi, $\nu = 0.2$) for which the bimaterial constant is $\epsilon = 0.066$ and $E^* = 1.6623 \times 10^7$ psi.

The J -integral (5) and the interaction integrals (26) are used to determine the energy release rate, \mathcal{G} and the stress intensity factors, K_I and K_{II} . The phase angle ψ is then obtained from (10), here $L = 2a$. The domain integrals are computed using several rectangular domains surrounding the crack tip. Excellent consistency, to within a fraction of a percent, between results obtained for each domain is observed (illustrating the domain-independence

Table 1. Comparison of numerical results (G, K_I, K_{II}, ψ) in their normalized forms with the analytical solution (30) for a penny-shaped interface crack under remote tension σ_0

	$\frac{\pi E^* \cosh^2(\pi \epsilon) G}{4 \sigma_0^2 a}$	$\frac{\sqrt{(\pi) \operatorname{Re}[\mathbf{K}(2a)^{\mu}]}}{2 \sigma_0 \sqrt{a}}$	$\frac{\sqrt{(\pi) \operatorname{Im}[\mathbf{K}(2a)^{\mu}]}}{2 \sigma_0 \sqrt{a}}$	ψ (radians)	$\frac{GE^* \cosh^2(\pi \epsilon)}{\mathbf{K}\mathbf{K}}$
Analytic (30)	1.0185	0.9969	0.1565	0.1557	1.000
Numerical	1.0105	0.9915	0.1566	0.1570	1.003
% error	-0.8%	-0.54%	0.06%	0.83%	0.3%

of the integrals). Normalized numerical and analytical results are shown in Table 1, where excellent agreement between the numerical and analytical results can be seen.

5.2. Longitudinal interface crack (fiber disbond)

Now consider a longitudinal interface crack such as found in fiber pull-out or disbond problems. The crack configuration is shown in Fig. 3(b) and a typical near crack-tip and details of the finite element mesh for the problem are shown in Fig. 5. Charalambides and Evans (1989) derived an analytical expression for the steady-state energy release along an axisymmetric longitudinal crack front, namely

$$\frac{\mathcal{G} E_f}{\sigma^2 R} = \frac{1}{4} \frac{\Sigma}{\Sigma + \frac{f}{1-f}}, \tag{31}$$

where $\Sigma = E_m/E_f$ and E_m and E_f are the Young's Moduli for the fiber and matrix respectively, R is the fiber radius, f is the fiber volume fraction and σ is the traction applied to the fiber at $z = 0$. This expression requires that the Poisson's ratios for each material be the same. The composite system consists of a single fiber surrounded by the matrix. The fiber/matrix system is taken to be infinite in extent in the z -direction and the fiber-matrix disbond takes the form of a semi-infinite longitudinal crack. The outer surface of the cylinder is taken to be traction free. The material parameters are $\Sigma = E_m/E_f = 0.4$ and $\nu = 0.25$, where ν is the Poisson's ratio of the matrix and the fiber. For the present numerical simulation of this configuration, the axial extent of the system is taken to be five times the crack length which in turn is taken to be large with respect to the fiber radius. Numerical checks are carried out to assure that steady-state conditions (i.e. no change in the normalized energy release rate with respect to crack length) have been achieved. For illustration, Figs 6(a), (b), (c) show the trends in the normalized energy release rate, the phase angle and the stress intensity factors as a function of the normalized crack (debond) length a/t for a fiber-volume

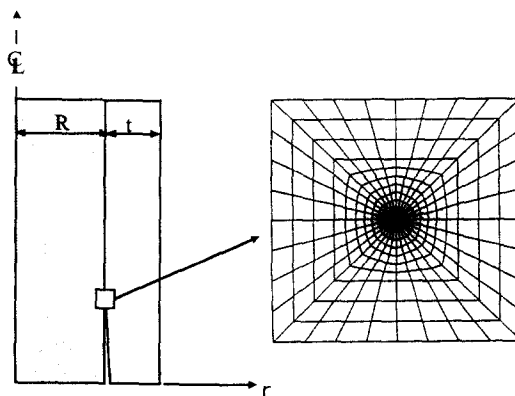


Fig. 5. Details of near crack-tip finite element mesh.

fraction $f = 0.9$. These trends clearly show that the steady-state conditions are reached simultaneously over a crack length of about $a = 10t \approx 0.55R$. It should be noted that once steady state is attained, there is no variation in either the energy release rate or the phase angle on further increase in crack length. In a similar study by Charalambides and Evans (1989) who used a stiffness derivative formulation, the trends in energy release rate and phase angle with the crack (debond) length show that while steady-state conditions are reached in the energy release rate, the phase angle does not attain a steady state.

Results are shown in Table 2 for various fiber volume fractions. For each fiber volume fraction, several domain paths are employed and the results are found to be very close and consistent. The numerical and analytical normalized energy release rates (31) are in close

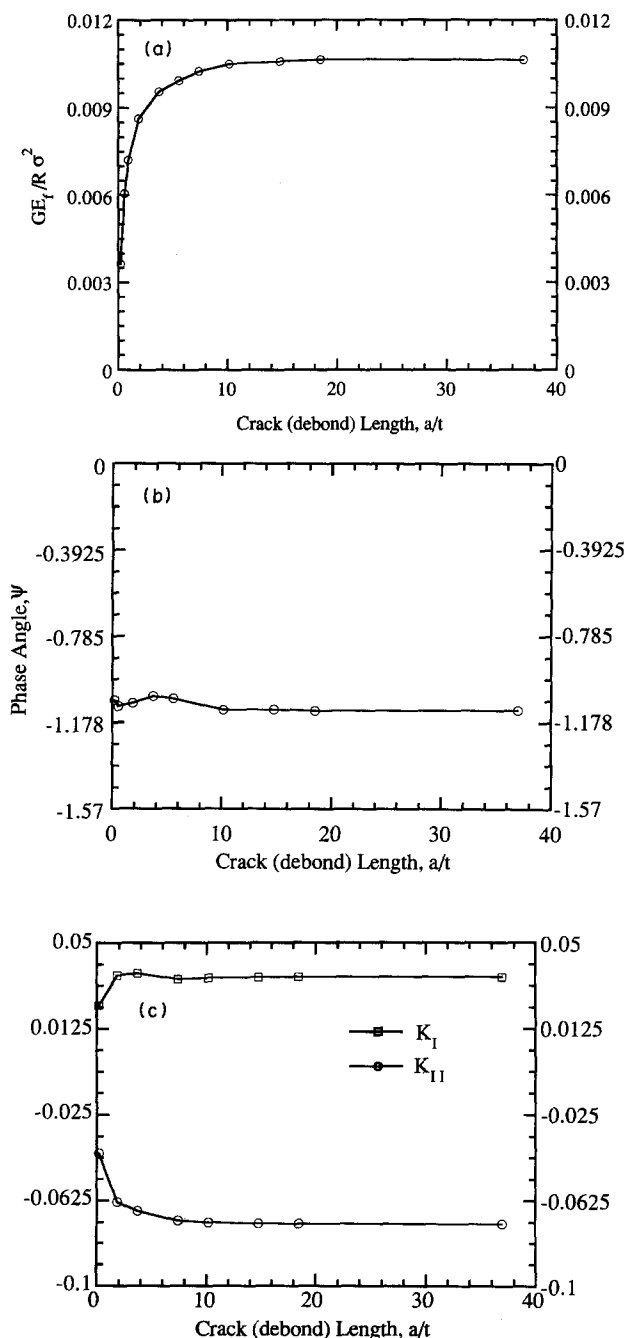


Fig. 6. Fiber disbond problem : (a) Normalized energy release rate $GE_t/\sigma^2 R$ as a function of debond crack length, a/t . (b) Phase angle ψ as a function of debond crack length, a/t . (c) The stress intensity factors, K_I and K_{II} as a function of debond crack length, a/t .

Table 2. The analytic and numerical energy release rates, the phase angle and the complex stress-intensity factors in their normalized form are tabulated for various fiber-volume fractions, f

f	$\frac{GE_f}{\sigma^2 R}$	$\frac{GE_f}{\sigma^2 R}$	$\text{Re}[KR^{*c}]$	$\text{Im}[KR^{*c}]$	ψ (radians)	$\frac{KR}{E^* \cosh^2(\pi e)}$	$\frac{E_f}{\sigma^2 R}$
	(31)	Numerical	$\sigma\sqrt{R}$	$\sigma\sqrt{R}$		$E^* \cosh^2(\pi e)$	$\sigma^2 R$
0.1	0.1956	0.1952	0.0495	0.3450	1.428		0.1952
0.2	0.1538	0.1535	0.0501	0.3044	1.408		0.1529
0.3	0.1207	0.1204	0.0507	0.2681	1.384		0.1196
0.4	0.0939	0.0936	0.0510	0.2349	1.357		0.0928
0.5	0.0714	0.0712	0.0509	0.2032	1.325		0.0705
0.6	0.0526	0.0524	0.0499	0.1725	1.289		0.0518
0.7	0.0366	0.0364	0.0473	0.1417	1.249		0.0358
0.8	0.0227	0.0226	0.0403	0.1097	1.222		0.0220
0.9	0.0106	0.0105	0.0351	0.0726	1.120		0.0105

agreement and plotted in Fig. 7(a). Also tabulated in Table 2 are the mixed-mode stress-intensity factors and the phase angle ψ (for length scale $L = R$) for various fiber-volume fractions f . As an additional check on the validity of the present formulation, the last column of Table 2 gives the energy release rate (in normalized form) calculated from the mixed mode stress intensity factors (16) and is seen to be consistent with the energy release rate computed numerically using (6).

6. CONCLUSIONS

Domain integral representations of crack-tip integrals for axisymmetric crack problems have been derived. The crack-tip integrals considered are the J -integral and the interaction

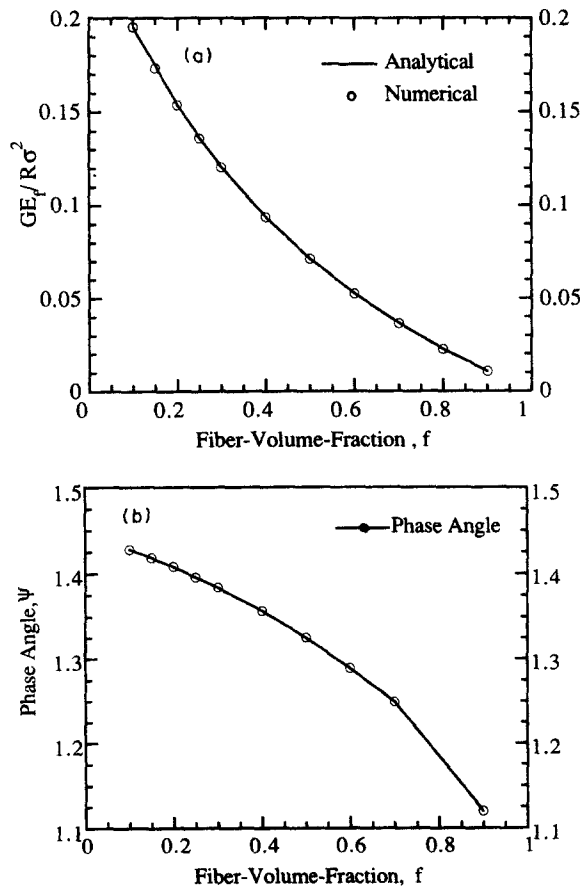


Fig. 7. Fiber disbond problem: (a) Normalized energy release rate $GE_f/\sigma^2 R$ as a function of fiber-volume fraction, f . (b) Phase angle ψ as a function of fiber-volume fraction, f .

energy integrals for mixed-mode crack problems with emphasis on interface cracks. The domain forms of the crack-tip integrals are specialized for two axisymmetric crack configurations namely, (a) a penny-shaped interface crack, and (b) a longitudinal interface crack. The latter configuration is that found in fiber pull-out problems. The present approach is shown to be an accurate and straightforward method for the numerical evaluation of fracture parameters in such axisymmetric interface fracture problems. The numerical examples illustrate that this method yields very accurate and consistent results for a general class of mixed-mode interface crack problems. Also the mixed-mode stress-intensity factors obtained are consistent with the energy-release rate evaluated through (6).

Charalambides and Evans (1989) noted some difficulties which arise in the specification of auxiliary fields for the extraction of mixed-mode stress-intensity factors using the stiffness derivative method. Consequently, they found it necessary to restrict the auxiliary fields to the finite elements in the immediate vicinity of the crack tip which might lead to inaccuracies. For example, it is observed that in their approach, the phase angles vary, even after the energy release rate has reached a steady state. Accuracy in this case, may require excessive numbers of elements in the near crack-tip region. It has been shown here that these difficulties arise due to the lack of equilibrium and compatibility of the chosen auxiliary fields in problems involving a curved three-dimensional crack front. With the domain integral method presented here, however, the auxiliary fields can be specified over the entire domain of interest. Although we have not pursued any extensive comparisons between the accuracy and efficiency of the two methods, the present approach may generally be expected to yield more accurate results for a given level of discretization or alternatively, reduce the near crack-tip mesh requirements.

In the derivation of the domain integral representations of the interaction energy integrals, the plane strain asymptotic fields are employed as the auxiliary fields in the pointwise definition of the interaction energy integrals. Since the plane strain fields are imposed on a curvilinear frame, both equilibrium and compatibility are violated and therefore the divergence of the interaction energy tensor \mathbf{P} does not vanish. The resulting contributions to the domain integral representations of the crack-tip integrals are seen to be qualitatively different from those which arise due to the presence of body forces or inhomogeneities, for example. Although in each case energy-momentum is not conserved, in the latter case this is due to the physical presence of body forces or inhomogeneities, while in the former it is solely a result of the mathematical formulation and the specification of the auxiliary fields along a curvilinear crack front.

The present method may also be extended in a similar fashion to the case of a general curvilinear crack front in three dimensions. Again, the auxiliary fields would be specified in the plane locally normal to the crack front and as a result, the interaction energy tensor \mathbf{P} would not be divergence-free. The resulting contributions to the domain-integrals could be determined following an analogous procedure to that outlined here. This approach may prove useful for the determination of mixed-mode stress intensity factors for surface breaking interface cracks and is the subject of ongoing research. Other areas where the present approach may prove useful is for mixed-mode and especially interface crack problems in shells.

Acknowledgements—The support of the Air Force Office of Scientific Research through contract No. AFSOR-90-0237 to Northwestern University is gratefully acknowledged.

REFERENCES

- Charalambides, P. G. and Evans, A. G. (1989). Debonding properties of residually stressed brittle-matrix composites. *J. Am. Ceramic Soc.* **72**, 746–753.
- Eshelby, J. D. (1956). The continuum theory of lattice defects. In *Solid State Physics* (Edited by F. Seitz and D. Turnbull), Vol. 3, pp. 79–141. Academic Press, New York.
- Eshelby, J. D. (1970). Energy relations and the energy momentum tensor in continuum mechanics. In *Inelastic Behavior of Solids* (Edited by M. F. Kanninen, W. F. Adler, A. R. Rosenfeld and R. T. Jaffee), pp. 77–114. McGraw-Hill, New York.
- Hutchinson, J. W. and Suo, Z. (1991). Mixed mode cracking in layered materials. In *Advances in Applied Mechanics* (Edited by J. W. Hutchinson and T. Y. Wu), Vol. 29, pp. 63–191. Academic Press, San Diego.

- Kassir, M. K. and Bregman, A. M. (1972). The stress intensity factor for a penny-shaped crack between two dissimilar materials. *J. Appl. Mech.* **39**, 308–310.
- Li, F. Z., Shih, C. F. and Needleman, A. (1985). A comparison of methods for calculating energy release rates. *Engng Fract. Mech.* **25**, 405–421.
- Moran, B. and Shih, C. F. (1987a). A general treatment of crack tip integrals. *Int. J. Fract.* **35**, 295–310.
- Moran, B. and Shih, C. F. (1987b). Crack tip and associated domain integrals from momentum and energy balance. *Engng Fract. Mech.* **27**, 615–642.
- Nakamura, T. (1991). Three-dimensional stress fields of elastic interface cracks. *J. Appl. Mech.* **58**, 939–946.
- Nakamura, T. and Parks, D. M. (1992). Determination of elastic T-stress along three-dimensional crack front using an interaction integral. *Int. J. Solids Structures* **29**(13), 1597–1611.
- Nikishkov, G. P. and Atluri, S. N. (1987). Calculation of fracture mechanics parameters for an arbitrary three-dimensional crack by the 'Equivalent Domain Integral Method'. *Int. J. Numer. Meth. Engng* **24**, 1801–1821.
- Rice, J. R. (1988). Elastic fracture mechanics concepts for interfacial cracks. *J. Appl. Mech.* **55**, 98–103.
- Rice, J. R., Suo, Z. and Wang, J. S. (1990). Mechanics and thermodynamics of brittle interfacial failure in bimaterial systems. In *Metal-Ceramic Interfaces* (Edited by M. Ruhle, A. G. Evans, M. F. Ashby and J. P. Hirth), pp. 269–294. Pergamon Press, Oxford.
- Shih, C. F. (1990). Cracks on bimaterial interfaces: elasticity and plasticity aspects. *Mater. Sci. Engng* **A143**, 77–90.
- Shih, C. F. and Asaro, R. J. (1988). Elastic-plastic analysis of cracks on bimaterial interfaces: Part I—Small scale yielding. *J. Appl. Mech.* **55**, 299–316.
- Shih, C. F., Moran, B. and Nakamura, T. (1986). Energy release rate along a three-dimensional crack front in a thermally stressed body. *Int. J. Fract.* **30**, 79–102.